Available online at www.sciencedirect.com
SCIENCE DIRECT®
Clinical Biomechanics 18 (2003) S17–S24
CLINICAL BIOMECHANICS
www.elsevier.com/locate/clinbiomech

# Effects of total contact insoles on the plantar stress redistribution: a finite element analysis

Weng-Pin Chen [a,*], Chia-Wei Ju [a], Fuk-Tan Tang [b]

[a] Department of Biomedical Engineering, Chung Yuan Christian University, Chungli 320, Taiwan, ROC
[b] Department of Rehabilitation, Chang Gung Memorial Hospital, Kweishan 333, Taiwan, ROC

**Abstract**

*Objective.* To investigate the effects of total contact insoles on the plantar stress redistribution using three-dimensional finite element analysis.

*Design.* The efficacies of stress reduction and redistribution of two total contact insoles with different material combinations were compared with those of a regular flat insole used as a baseline condition.

*Background.* Many specially designed total contact insoles are currently used to reduce the high plantar pressure in diabetic patients. However, the design of total contact insoles is mostly empirical and little scientific evidence is available to provide a guideline for persons who prescribe such insoles.

*Methods.* To use three-dimensional finite element models of the foot together with insoles to investigate the effects of total contact insoles on the foot plantar pressure redistributions. Nonlinear foam material properties for the different insole materials and the contact behavior in the foot–insole interface were considered in the finite element analysis.

*Results.* Results showed that the peak and the average normal stresses were reduced in most of the plantar regions except the midfoot and the hallux region when total contact insoles were worn compared with that of the flat insole condition. The reduction ratios of the peak normal stress ranged from 19.8% to 56.8%.

*Conclusions.* Finite element analysis results showed that the two sets of total contact insoles used in the current study can both reduce high pressures at regions such as heel and metatarsal heads and can redistribute the pressure to the midfoot region when compared with the flat insole condition.

**Relevance**

It is possible to simulate foot deformities, change in material properties, different ambulatory loading conditions, and different orthotic conditions by altering the finite element model in a relatively easy manner and these may be of interests to the medical professionals who treat foot-related problems.


*Keywords:* Plantar pressure; Total contact insole; Finite element analysis; Diabetic neuropathy; Foot orthosis

## 1. Introduction

It has been pointed out by many researchers that the biomechanical factors play a crucial role in the aetiology, treatment, and prevention of diabetic foot ulcers (Boulton et al., 1984; Boulton et al., 1983; Caputo et al., 1994; Cavanagh et al., 1996). The peripheral neuropathy in diabetic patients often leads to the loss of sensation, weakness of foot muscle strength, and foot ulceration. Many specially designed therapeutic footwear or orthoses are currently used to reduce the high plantar pressure in diabetic patients (Boulton et al., 1984; Brown et al., 1996; Donaghue et al., 1996; Kato et al., 1996; Lavery et al., 1996; Lord and Hosein, 1994; Reiber et al., 1997). Among them the total contact insoles (TCI) are commonly used. They are insoles custom-molded according to the plantar geometry of the patient's foot in order to provide accommodative support, and to redistribute and reduce high plantar pressures under the heel and the metatarsal regions. Although its efficacy has been reported in previous clinical follow-up studies and in-shoe pressure measurement studies (Boulton et al.,

* Corresponding author.
*E-mail address:* wpchen@cycu.edu.tw (W.-P. Chen).

0268-0033/03/$ - see front matter © 2003 Elsevier Science Ltd. All rights reserved.
doi:10.1016/S0268-0033(03)00080-9

1984; Cavanagh et al., 1996; Kato et al., 1996; Lord and Hosein, 1994); the design of TCI is mostly empirical and little scientific evidence is available to provide a guideline for persons who prescribe such insoles.

Currently there are many commercially available insole materials, but there is limited information on the effects of stress redistribution of insoles with different combinations of materials and thicknesses. Therefore, further investigation is necessary. Currently, there are two feasible approaches to quantifying foot pressure. One approach employs the well-established in-shoe measuring techniques to obtain plantar pressure during gait with different insole combinations (Boulton et al., 1983; Alexander et al., 1990; Cobb and Claremont, 1995; Hosein and Lord, 2000; Lord et al., 1992). However, this approach is time-consuming and a large number of measurements need to be performed on different subjects with different insole combinations in order to obtain statistically significant results. The other approach is to use the finite element method to model the foot–insole structure and to analyze the effects of different insole combinations on the plantar stress distributions. This approach has the benefit of allowing modification of different insole combinations and performing parametric analysis with a relatively quick and easy procedure.

Finite element method has been employed previously in many foot-related biomechanics studies (Yettram and Camilleri, 1993; Chu et al., 1995; Jacob et al., 1996). In 1997, Lemmon et al. (1997) investigated the effect of therapeutic footwear insole thickness on the plantar pressure using a 2-D plane strain finite element model. In their study, only the second metatarsal head region of the foot was modeled, therefore, no overall plantar pressure distribution was available. It has been demonstrated that the finite element method can be a promising means for predicting the stress distributions in the foot–insole interface if the complex geometry and material conditions of the foot and insole are properly taken into account.

The present study investigated the effects of TCI on the foot plantar pressure redistributions using three-dimensional finite element models of the foot together with insoles. The efficacies of stress reduction and redistribution of two sets of TCI with different material combinations were compared with those of a regular flat insole. Nonlinear foam material properties of different insole materials and the contact behavior in the foot–insole interface were considered in the finite element analysis.

## 2. Methods

### 2.1. Finite element model generation

A three-dimensional finite element model of a 24-year-old male subject's right foot was generated according to the procedures described previously (Chen et al., 2001). The finite element pre- and post-processing program—Mentat II V.3.2 (MSC, Los Angeles, CA, USA) was employed to generate the finite element foot model. The foot bone model with cartilage elements and major plantar ligaments is shown in Fig. 1A. Five 2-node cable elements connecting the plantar side of each of the five metatarsal heads and the calcaneus were created to represent the plantar aponeurosis. Three 2-node cable elements connecting the plantar side of the cuboid and the calcaneus were created to simulate the short plantar ligaments. The complete foot model of the bone and soft tissue elements is shown in Fig. 1B. The element types and numbers used for each part of the foot model are listed in Table 1.

The finite element models for a common flat insole and two sets of specially designed TCI were created directly underneath the foot model. The flat insole was made of Microcel Puff with a thickness of 6.5 mm (as shown in Fig. 2A). The first set of TCI (TCI-1) consisted of three layers: top layer is PPT (3.2 mm thick), mid layer is Microcel Puff (6.5 mm thick) and the bottom layer is Thermocork (11.6 mm thick). The TCI was custom-molded according to the plantar geometry of the foot. Therefore, the finite element mesh for the TCI-1 was created by expanding outward from the plantar surface elements of the foot and is shown in Fig. 2B. The second set of TCI (TCI-2) consisted of two layers: top

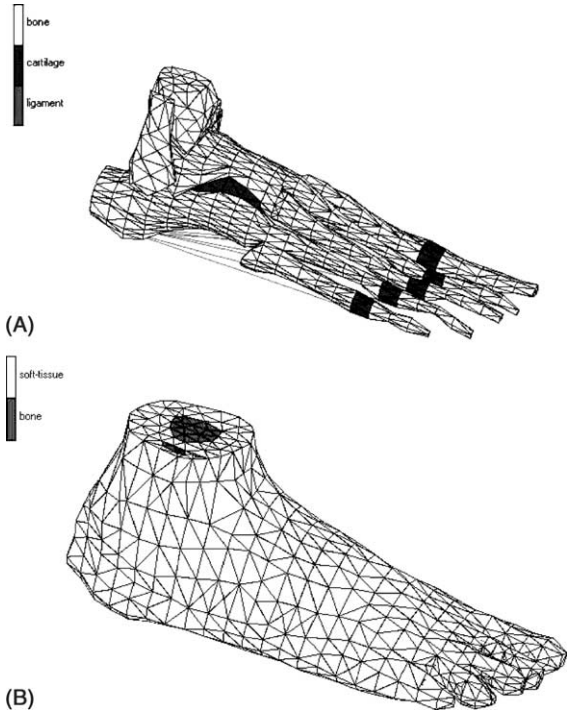


Fig. 1. Finite element models of (A) the foot bones with cartilage and major plantar ligaments, and (B) the complete model of the foot with soft tissues.

Table 1
Element type, number of elements, cross-sectional area, modulus of elasticity, and Poisson's ratio used for each of the materials in the finite element model

| Material | Element type | No. of elements | Cross-sectional area ($cm^2$) | Modulus of elasticity | Poisson's ratio ($v$) |
|---|---|---|---|---|---|
| Bone | 4-node tetrahedron | 4574 | – | 10 GPa | 0.34 |
| Soft tissue | 4-node tetrahedron | 9630 | – | 1.15 MPa | 0.49 |
| Cartilage | 4-node tetrahedron | 468 | – | 10 MPa | 0.4 |
| Ligament | 2-node cable | 8 | 3.16 | 11.5 MPa | – |
| Flat insole | 6-node wedge | 378 | – | – | – |
| TCI-1 | 6-node wedge | 1260 | – | – | – |
| TCI-2 | 6-node wedge | 840 | – | – | – |

layer is medium Plastazote (6.4 mm thick), and the bottom layer is PPT (12.7 mm thick). The finite element mesh for the TCI-2 is shown in Fig. 2C. The flat insole, TCI-1, and TCI-2 meshes were then merged with the foot model, respectively. The interface between the foot plantar region and the insole was considered to be discontinuous and contact bodies were assumed for the foot and the insole.

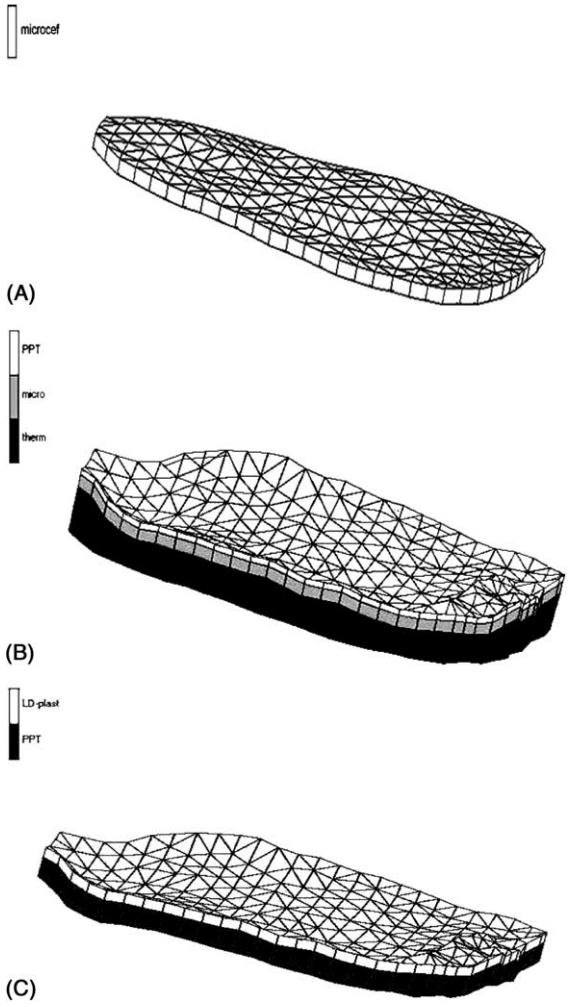


Fig. 2. Finite element models of the (A) flat insole (consisted of Microcel Puff), (B) TCI-1 (consisted of PPT, Microcel Puff and Thermocork), and (C) TCI-2 (consisted of medium Plastazote and PPT).

### 2.2. Material properties

The bone and soft tissue elements of the foot were assumed to be linear, elastic solids. The material properties (modulus of elasticity and Poisson's ratio) for the bone, soft tissue, cartilage, and ligament elements are listed in Table 1. The insole materials are polymers that possess nonlinear elastic stress–strain behavior. The term elastomer is often used to refer to material that possesses a rubber-like behavior. The material properties for the insole materials used in this study are not currently available from the manufacturers. Therefore, compression tests were performed based on the ASTM D575-91 test method (Standard test methods for rubber properties in compression) on an Instron 8511 material-testing machine (Instron, Canton, MA, USA). Five circular specimens were made for each of the insole materials and compression tests were performed using a displacement control of 12 mm/min. The average stress–strain curve for the five specimens were calculated and input to the curve-fitting program in the Mentat II V.3.2 software for determining the nonlinear foam material coefficients. Fig. 3 shows the averaged stress–strain curve from the five specimens (input) and the calculated stress–strain curve for the medium Plastazote displayed in the curve-fitting program. The rubber foam material type provided by the MARC K.7.3 finite element software (MSC, Los Angeles, CA, USA) was used to model the insole materials. The strain energy form for the foam material can be represented as:

$$W = \sum_{n=1}^{N} \frac{\mu_n}{\alpha_n}(\lambda_1^{\alpha_n} + \lambda_2^{\alpha_n} + \lambda_3^{\alpha_n} - 3) + \sum_{n=1}^{N} \frac{\mu_n}{\alpha_n}(1 - J^{\beta_n}) \quad (1)$$

where $\mu_n$ are the material modulus, $\alpha_n$ are the deviatoric exponents, $\beta_n$ are the volumetric exponents, $\lambda_1$, $\lambda_2$, $\lambda_3$ are the principal stretch ratios, $J$ is the Jacobian, and $N$ is the number of order as described in the MARC K.7.3 Theory Manual (MARC, 1997). The foam material coefficients for the PPT, medium Plastazote, Microcel Puff, and Thermocork are calculated from experimental data

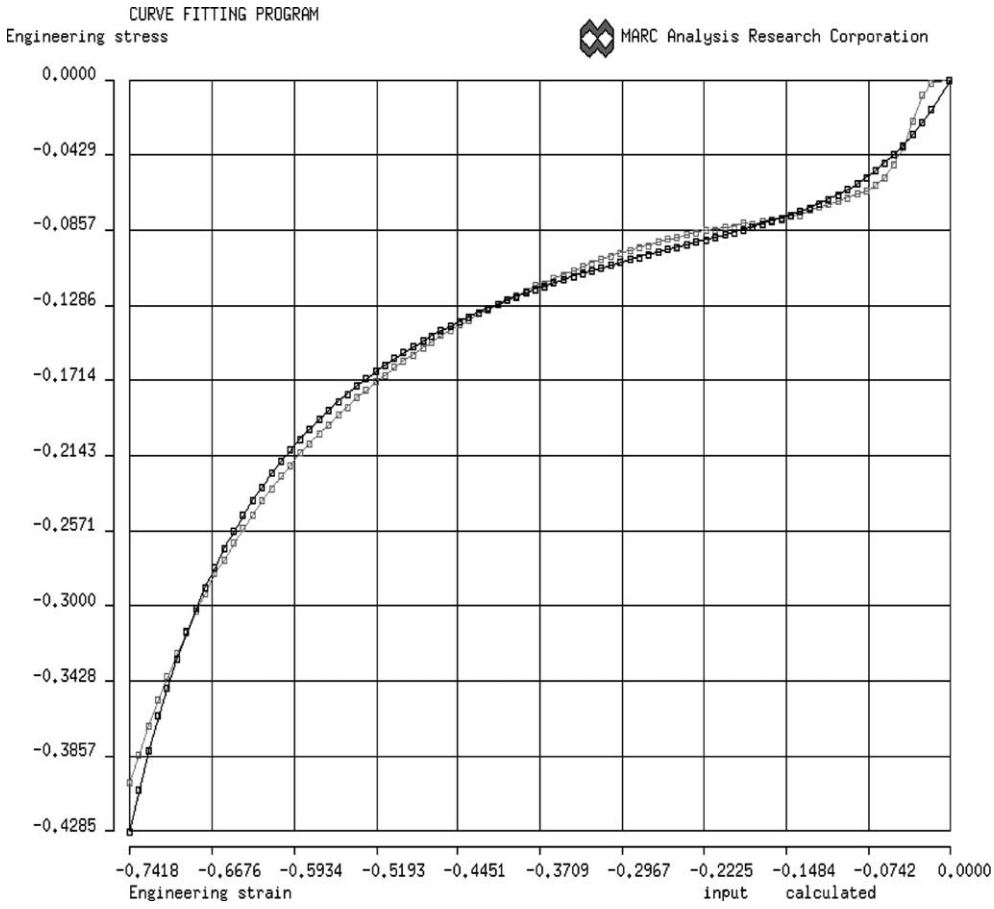


Fig. 3. The original and the calculated stress–strain curves for the medium Plastazote insole material displayed in the curve-fitting program.

and shown in Table 2. The number of order ($N$) used for each material was determined by the curve-fitting program.

### 2.3. Loading and boundary conditions

Although the foot can be subjected to very diverse loading conditions under different ambulatory activities, in the current study we only considered the normal gait during mid-stance phase. The forces and moments applied on the plantar surface of the foot during gait can be measured using force platform. However, if such forces and moments were applied directly to the plantar foot surface, there would be stress concentrations at the points of load application on the foot plantar surface. Therefore, instead of direct application of loads on the foot, an alternative approach for the loading condition was used in this study. We assume the foot to be steady and the floor to be a rigid plane moving towards the foot with constant velocity. A rigid plane simulating the floor was created 10 mm beneath and parallel to the foot–insole model and set to be moving towards the model at

Table 2
Foam material coefficients calculated from the curve-fitting program for each of the insole materials

| Material | Material coefficients | | | |
|---|---|---|---|---|
| | $n$ | $\mu_n$ | $\alpha_n$ | $\beta_n$ |
| PPT | $n=1$ | $\mu_1=0.062$ | $\alpha_1=15.000$ | $\beta_1=-14.558$ |
| | $n=2$ | $\mu_2=-0.006$ | $\alpha_2=-5.000$ | $\beta_2=4.8529$ |
| Medium plastazote | $n=1$ | $\mu_1=0.070$ | $\alpha_1=16.325$ | $\beta_1=-12.244$ |
| | $n=2$ | $\mu_2=-0.002$ | $\alpha_2=-2.002$ | $\beta_2=1.501$ |
| Microcel puff | $n=1$ | $\mu_1=0.167$ | $\alpha_1=22.882$ | $\beta_1=-2.860$ |
| Thermocork | $n=1$ | $\mu_1=0.369$ | $\alpha_1=44.072$ | $\beta_1=-5.509$ |

a constant velocity of 20 mm/s. The foot and the insoles were assumed to be deformable contact bodies while the floor was assumed to be a rigid contact plane. An assumed friction coefficient of 0.3 was used for both the foot–insole and the insole–floor interfaces.

In the finite element analysis, a quasi-static displacement control of the rigid plane was employed instead of the often-used load control. In this study, we only simulated gait during mid-stance phase (total loading time is 0.12 s, total displacement is 2.4 mm). The nodes on the proximal tibial surface of the foot and the nodes on the anterior and posterior edges of the insoles were constrained in all directions as boundary condition to prevent rigid body motion.

### 2.4. Finite element analysis

After the material properties and the boundary conditions were set up in each of the three foot–insole models, finite element analyses were performed using MARC K.7.3 on an HP SPP/2000 supercomputer (Hewlett-Packard, Palo Alto, CA, USA) at the National Center for High-Performance Computing (NCHC, Hsinchu, Taiwan). The analysis results were retrieved back to a local SGI Indy-R5000 workstation (Silicon Grahpics, Mountain View, CA, USA) for the post-processing of the stress distributions at the foot–insole interfaces.

## 3. Results

The normal stress distributions on the foot plantar surface for wearing the flat insole, TCI-1, and TCI-2 models are illustrated by gray-scale plots in Fig. 4A–C, respectively. The normal plantar stresses are mostly compressive (negative values), therefore, the stress fringe bar displayed in Fig. 4 ranges from 0 to −1 MPa (−1000 KPa). As seen from the stress distributions for the flat insole model (Fig. 4A), high compressive stresses were found on the plantar surface under the metatarsal heads and the heel regions. When TCI were worn, the high plantar stresses were redistributed to the midfoot region and reduced significantly as seen in Fig. 4B and C, respectively. In order to understand the effects of force produced by the pushing of a rigid plane, the total reaction forces at the constrained tibial surface nodes for each of the three models (flat, TCI-1, and TCI-2) were calculated and found to be 572.6, 697.5, and 647.3 N, respectively.

In order to compare the plantar stresses in a quantitative way, the foot plantar surface was divided into seven regions, namely: heel, midfoot, first MT (metatarsal), second MT, other MT, hallux, and other toes. The peak normal stresses and the average normal stresses at each of the seven regions were found and

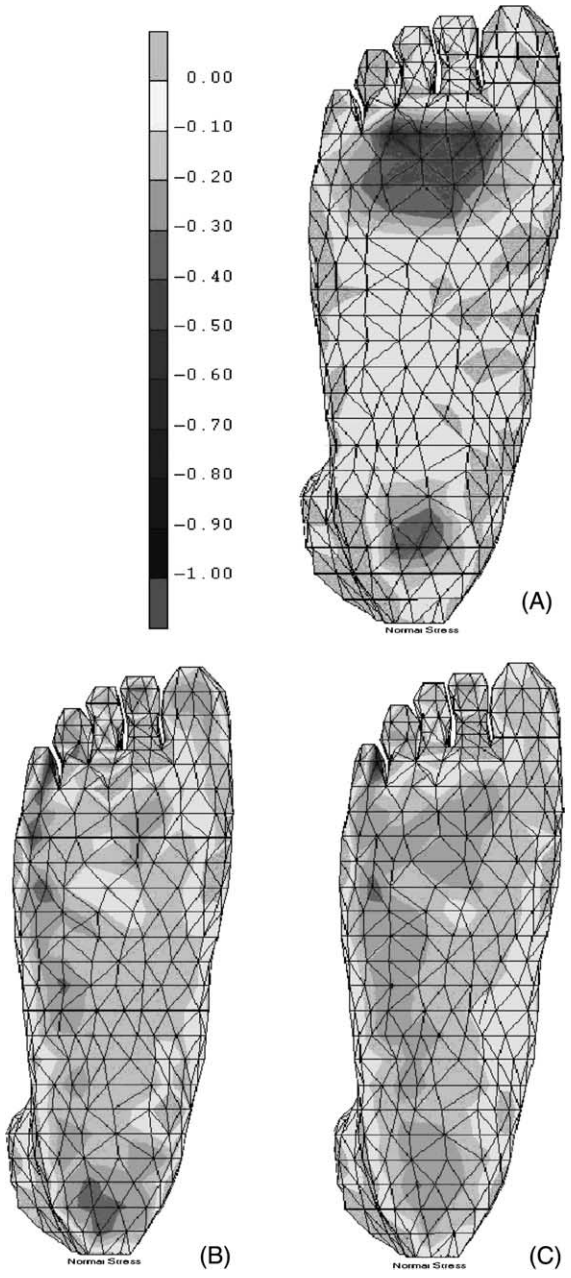


Fig. 4. Normal stress distributions on the plantar surface for wearing the (A) flat insole, (B) TCI-1, and (C) TCI-2 (Unit: MPa).

calculated for the three models (flat insole, TCI-1, and TCI-2) and compared in Figs. 5 and 6. The peak normal stresses for the TCI-1 and TCI-2 were reduced in all regions except for the midfoot region. The average normal stresses for the TCI-1 and TCI-2 were also reduced in all regions except for the midfoot and the hallux regions. This observation showed that both the TCI can effectively reduce the high plantar pressures on the heel and the metatarsal regions and redistribute the pressure to the midfoot region.

The change ratios of the peak and average normal stresses for the TCI-1 and TCI-2 in comparison with

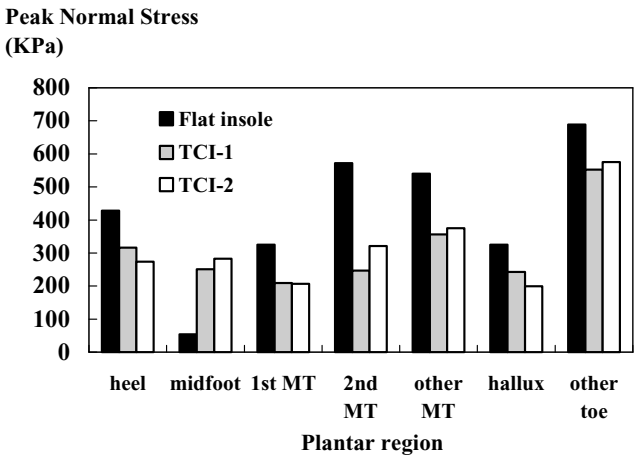


Fig. 5. Peak normal stresses on each of the foot plantar regions for wearing the flat insole, TCI-1, and TCI-2.

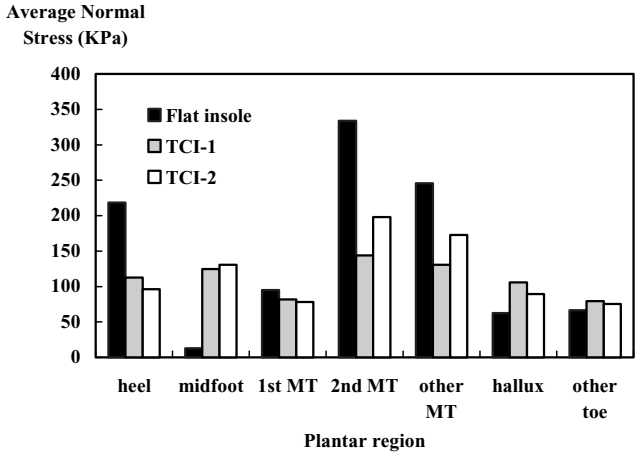


Fig. 6. Average normal stresses on each of the foot plantar regions for wearing the flat insole, TCI-1, and TCI-2.

those of the baseline flat insole condition were calculated and shown in Table 3, where positive values represent stress increase while negative values represent stress reduction. The peak and average normal stresses were reduced in most of the plantar regions when TCI were worn compared with those of the flat insole condition except that the peak normal stresses increased at the midfoot region (365.7% for TCI-1 and 425.0% for TCI-2) and the average normal stresses increased at the midfoot region (874.3% for TCI-1 and 921.8% for TCI-2), the hallux region (69.6% for TCI-1 and 43.0% for TCI-2), and the other toes region (19.4% for TCI-1 and 13.1% for TCI-2). The reduction ratios of the peak normal stress for TCI-1 compared with those of the flat insole ranged from 19.8% (other toes) to 56.8% (second MT). The reduction ratios of the average normal stress for TCI-1 compared with those of the flat insole ranged from 14.1% (first MT) to 56.8% (second MT). The reduction ratios of the peak normal stress for TCI-2 compared with those of the flat insole ranged from 16.5% (other toes) to 43.8% (second MT). The reduction ratios of the average normal stress for TCI-2 compared with those of the flat insole ranged from 18.0% (first MT) to 55.9% (heel). Both the second MT and the heel regions are the most significant pressure relieved regions on the plantar surface.

## 4. Discussion

In this study, a computational approach using the finite element method was proposed for investigating of the effects of stress redistribution of TCI. The analysis results showed that when TCI were used, the peak and the average normal plantar pressures were both reduced in the high pressure regions (metatarsal heads and heel). The high pressures were redistributed to the midfoot region. Similar results were reported by Lord and Hosein (1994) who used pressure-measuring insole systems. In their study, custom-molded inserts used in the orthopedic shoes of diabetic patients at risk of plantar ulceration were compared with flat inserts. They found that the pressure was reduced significantly with the use of molded inserts (flat inserts: $305 \pm 79$ kPa; molded inserts: $216 \pm 70$ kPa; $n = 6$, $p < 0.005$). Kato et al. (1996) investigated the effects of foot orthoses on the distribution of plantar pressures using a pressure-sensitive insole in seven diabetic patients (13 feet). They found that the pre-orthotic peak pressure was

Table 3
The change ratios of the peak and the average normal plantar pressures for wearing the TCI-1 and the TCI-2 compared to the flat insole condition at seven different plantar regions

| | TCI-1 | | TCI-2 | |
|---|---|---|---|---|
| | Peak (%) | Average (%) | Peak (%) | Average (%) |
| Heel | −26.1 | −48.4 | −35.9 | −55.9 |
| Midfoot | 365.6 | 874.3 | 425.0 | 921.8 |
| First MT | −35.6 | −14.1 | −36.3 | −18.0 |
| Second MT | −56.8 | −56.8 | −43.8 | −40.7 |
| Other MT | −34.0 | −46.9 | −30.5 | −29.7 |
| Hallux | −25.2 | 69.6 | −38.5 | 43.0 |
| Other toes | −19.8 | 19.4 | −16.5 | 13.1 |

$130.6 \pm 41.9$ kPa, while the post-orthotic peak pressure was reduced to $52.6 \pm 17.9$ kPa. The mean reduction of pressure was 56.3%. Brown et al. (1996) used the FSCAN in-shoe pressure measuring system to determine the efficacy of pressure redistribution with Plastazote, Spenco, cork, and plastic foot orthoses as compared with that of the control (no orthosis). They concluded that Plastazote, cork, and plastic foot orthoses could be beneficial in relieving pressure in certain regions of the shoe–foot interface, but at the cost of increasing pressure in other areas of the plantar surface. There were no statistically significant changes in peak pressure between the orthotic and control conditions in the great toe, first metatarsal head, second through fifth toes, or total foot regions. Decreases in peak pressure were found in the forefoot, heel, and second through fifth metatarsal head regions when orthoses were worn. The average peak pressure ranges for the orthotic and control conditions at the three highest-pressure regions were: forefoot (1002–1126 kPa), heel (765–863 kPa), second through fifth metatarsal heads (383–453 kPa). These peak pressure values were higher than those reported in the previous studies by Lord and Hosein (1994) and Kato et al. (1996).

It is not surprising to find the wide range of variations in peak pressures reported in various plantar pressure measurement studies due to the possible variations between measuring techniques, subjects, gait patterns, and orthoses. Our finite element results showed similar trends of pressure distributions of the high plantar pressure regions and the pressure values were within the range of previously reported pressure values. Also the pressure relief effects at the heel and the metatarsal regions and the pressure increase effects at the midfoot region for the TCI corresponded well with those reported in previous experimental studies.

A number of assumptions were made in the current finite element analysis. The material properties for the foot bone, soft tissue, cartilage, ligaments were assumed to be homogeneous, linear, and elastic solids. In the future, the nonlinear, viscoelastic, and anisotropic material properties for the foot tissues may be considered when such material properties become available. The geometry of the foot model was created according to the CT images from a healthy person. However, it has been reported in literature (Cavanagh et al., 1996; Lemmon et al., 1997) that the foot bone structure and the plantar soft tissue material properties for diabetic patients with neuropathy may be significantly different from those for normal persons. Therefore, in the future, foot deformity and the variations in plantar soft tissue thickness and material properties for diabetic patients could be further investigated. It has also been reported in literature (Zhu et al., 1991; Rozema et al., 1996) that the plantar pressures may increase significantly during various ambulatory activities of daily living, such as, slow and fast walking, running, stair climbing, and rising from a chair. Therefore, other ambulatory loading conditions should be considered besides the mid-stance during normal gait considered in the current study.

The two sets of TCI (TCI-1 and TCI-2) used in the current study were created arbitrarily according to the suggestion of foot orthotist. Results showed that the TCI can both reduce high pressures at the forefoot and heel regions and redistribute the pressure to the midfoot region. It is hard to conclude which TCI performs better than the other from the current results. A more specific criterion for comparing the pressure-relieving effects should be established in the future. Further parametric studies could be conducted to investigate the effects of different insole material combinations and thickness on the reduction and redistribution of the foot plantar pressures. It is hoped that a design guideline or rationale can be provided to the persons who prescribe and fabricate the total contact insoles or orthoses for diabetic neuropathic patients.

## 5. Conclusion

Finite element analysis results showed that the two sets of TCI used in the current study can both reduce high pressures at regions such as heel and metatarsal heads and can redistribute the pressure to the midfoot region when compared with the flat insole condition. The finite element foot–insole models can provide a feasible means for investigating plantar pressure distributions of the foot subjected to the intervention of custom-molded, TCI. It has the benefit of comparing the effects of pressure distributions for different insole conditions on the same basis (foot geometry, material property, and loading condition). Also it is possible to simulate foot deformities, change in material properties, different ambulatory loading conditions, and different orthotic conditions by altering the finite element model in a relatively easy manner and these may be of interest to the medical professionals who treat foot-related problems.

## Acknowledgements

This study was supported by the grant from the National Science Council of the Republic of China (grant no. NSC-89-2614-E-033-001). The computing facilities provided by the National Center for High-Performance Computing are greatly appreciated.

## References

Alexander, I.J., Chao, E.Y.S., Johnson, K.A., 1990. The assessment of dynamic foot-to-ground contact forces and plantar pressure

distribution: a review of the evolution of current techniques and clinical applications. Foot Ankle Int. 11, 152–167.

Boulton, A.J.M., Franks, C.I., Betts, R.P., Duckworth, T., Ward, J.D., 1984. Reduction of abnormal foot pressures in diabetic neuropathy using a newpolymer insole material. Diabetes Care 7, 42–46.

Boulton, A.J.M., Hardisty, C.A., Betts, R.P., Franks, C.I., Worth, R.C., Ward, J.D., et al., 1983. Dynamic foot pressure and other studies as diagnostic and management aids in diabetic neuropathy. Diabetes Care 6, 26–33.

Brown, M., Rudicel, S., Esquenazi, A., 1996. Measurement of dynamic pressures at the shoe–foot interface during normal walking with various foot orthoses using the FSCAN system. Foot Ankle Int. 17, 152–156.

Caputo, G.M., Cavanagh, P.R., Ulbrecht, J.S., Gibbons, G.W., Karchmer, A.W., 1994. Assessment and management of foot disease in patients with diabetes. New Engl. J. Med. 331, 854–860.

Cavanagh, P.R., Ulbrecht, J.S., Caputo, G.M., 1996. Biomechanical aspects of diabetic foot disease: aetiology, treatment, and prevention. Diabetic Med. 13, S17–S22.

Chen, W.P., Tang, F.T., Ju, C.W., 2001. Stress distribution of the foot during mid-stance to push-off in barefoot gait: a 3-D finite element analysis. Clin. Biomech. 16, 614–620.

Chu, T.M., Reddy, N.P., Padovan, J., 1995. Three-dimensional finite element stress analysis of the polypropylene, ankle-foot orthosis: static analysis. Med. Eng. Phys. 5, 372–379.

Cobb, J., Claremont, D.J., 1995. Transducers for foot pressure measurement: survey of recent developments. Med. Biol. Eng. Comput. 33, 525–532.

Donaghue, V.M., Sarnow, M.R., Giurini, J.M., Chrzan, J.S., Habershaw, G.M., Veves, A., 1996. Longitudinal in-shoe foot pressure relief achieved by specially designed footwear in high risk diabetic patients. Diabetes Res. Clin. Pr. 31, 109–114.

Hosein, R., Lord, M., 2000. A study of in-shoe plantar shear in normals. Clin. Biomech. 15, 46–53.

Jacob, S., Patil, K.M., Braak, L.H., Huson, A., 1996. Stresses in a 3D two arch model of a normal human foot. Mech. Res. Commun. 23, 387–393.

Kato, H., Takada, T., Kawamura, T., Hotta, N., Torii, S., 1996. The reduction and redistribution of plantar pressures using foot orthoses in diabetic patients. Diabetes Res. Clin. Pr. 31, 115–118.

Lavery, L.A., Lavery, D.C., Vela, S.A., Quebedeaux, T.L., 1996. Reducing dynamic foot pressures in high-risk diabetic subjects with foot ulcerations. Diabetes Care 19, 818–821.

Lemmon, D., Shiang, T.Y., Hashmi, A., Ulbrecht, J.S., Cavanagh, P.R., 1997. The effect of insoles in therapeutic footwear—a finite element approach. J. Biomech. 30, 615–620.

Lord, M., Hosein, R., 1994. Pressure redistribution by molded inserts in diabetic footwear: A pilot study. J. Rehab. Res. Dev. 31, 214–221.

Lord, M., Hosein, R., Williams, R.B., 1992. Method for in-shoe shear stress measurement. J. Biomed. Eng. 14, 181–186.

MARC Volume A: Theory and User Information, Version K7, MARC Analysis Research Corp., Palo Alto, CA, USA, 1997.

Reiber, G.E., Smith, D.G., Boone, D.A., del Aguila, M., Borchers, R.E., Mathews, D., et al., 1997. Design and pilot testing of the DVA/Seattle footwear system for diabetic patients with foot insensitivity. J. Rehab. Res. Dev. 34, 1–8.

Rozema, A., Ulbrecht, J.S., Pammer, S.E., Cavanagh, P.R., 1996. In-shoe plantar pressures during activities of daily living: implications for therapeutic footwear design. Foot Ankle Int. 17, 352–359.

Yettram, A.L., Camilleri, N.N., 1993. The forces acting on the human calcaneus. J. Biomed. Eng. 15, 46–50.

Zhu, H., Wertsch, J.J., Harris, G.F., Loftsgaarden, J.D., Price, M.B., 1991. Foot pressure distribution during walking and shuffling. Arch. Phys. Med. Rehab. 72, 390–397.